

Role of streams in myxobacteria aggregate formation

Maria A Kiskowski^{1,3}, Yi Jiang² and Mark S Alber¹

¹ Departments of Mathematics and Center for the Study of Biocomplexity, 255 Hurley Building, University of Notre Dame, Notre Dame, IN 46556-4618, USA

² Theoretical Division, MS B284, Los Alamos National Laboratory, Los Alamos, NM 87545, USA

E-mail: malber@nd.edu

Received 25 June 2004

Accepted for publication 20 September 2004

Published 29 October 2004

Online at stacks.iop.org/PhysBio/1/173

doi:10.1088/1478-3967/1/3/005

Abstract

Cell contact, movement and directionality are important factors in biological development (morphogenesis), and myxobacteria are a model system for studying cell–cell interaction and cell organization preceding differentiation. When starved, thousands of myxobacteria cells align, stream and form aggregates which later develop into round, non-motile spores. Canonically, cell aggregation has been attributed to attractive chemotaxis, a long range interaction, but there is growing evidence that myxobacteria organization depends on contact-mediated cell–cell communication. We present a discrete stochastic model based on contact-mediated signaling that suggests an explanation for the initialization of early aggregates, aggregation dynamics and final aggregate distribution. Our model qualitatively reproduces the unique structures of myxobacteria aggregates and detailed stages which occur during myxobacteria aggregation: first, aggregates initialize in random positions and cells join aggregates by random walk; second, cells redistribute by moving within transient streams connecting aggregates. Streams play a critical role in final aggregate size distribution by redistributing cells among fewer, larger aggregates. The mechanism by which streams redistribute cells depends on aggregate sizes and is enhanced by noise. Our model predicts that with increased internal noise, more streams would form and streams would last longer. Simulation results suggest a series of new experiments.

1. Introduction

Traditionally, models for aggregation in biology have been based on attractive chemotaxis, a long range cell–cell interaction that shares many features of chemical reaction-diffusion dynamics. Examples include bacteria, e.g. *E. coli* (Tsimring *et al* 1995, Brenner *et al* 1998) and *B. subtilis* (Matsushita and Fujikawa 1990, Ben-Jacob *et al* 2000; Komoto *et al* 2003) and amoebae, e.g. *Dictyostelium discoideum* (Martiel and Goldbeter 1987, Höfer *et al* 1995, Ben-Jacob *et al* 2000). Chemotactic signals play an important role in the initial position of aggregates (Tsimring *et al* 1995; Wakano *et al* 2003), and subsequent signaling biases cell

motion toward developing aggregates (Tsimring *et al* 1995). Cells following the maximal chemical gradient navigate toward aggregates that are both large and near.

At the same time, cell contact, movement and directionality are important factors in biological development (morphogenesis). Sub-groups of cells align within tissues and cells with different orientations within a tissue may differentiate into distinct cell types (Alber *et al* 2003). Cells may interact via specialized parts of their cell body and are sensitive to the density of cells around them (Alber *et al* 2004a). In these contexts, cells respond to short-range interactions, and patterns are self-organized rather than a response to externally imposed signals (Ben-Jacob and Levine 1988, Newman 1988).

Myxobacteria are a model system for studying cell–cell interaction and cell organization preceding differentiation, because there is growing evidence that

³ Current address: Biomathematics Study Group, Department of Mathematics, Stevenson Center, Vanderbilt University, Nashville, TN, USA.

myxobacteria organization depends on contact-mediated cell–cell communication rather than on long-range chemotactic cues (Dworkin 1996, Lobedanz 2003, Sjøgaard-Andersen 2003, Kaiser 2003). Myxobacteria are rod-shaped, gliding bacteria. When starved, cells align, stream, and form aggregates that later develop into mature fruiting bodies, a three-dimensional structure within which cells differentiate into round, non-motile spores.

There are several intriguing questions regarding aggregation in myxobacteria. How do individual myxobacteria cells find their way to developing aggregates without using an externally imposed signal? Myxobacteria have been observed to travel large distances to enter an aggregate, bypassing closer aggregates on their route (Jelsbak and Sjøgaard-Andersen 2000). Further, how do myxobacteria cells using only short-range communications ensure that they have formed large, well-spaced aggregates?

We demonstrate that a model for aggregation, introduced in Alber *et al* (2004b) and based on simplified assumptions for cell shape and aligned motion, can account for many experimental observations and shed light on these questions. Our model qualitatively reproduces not only the sequence of stages which occur during myxobacteria aggregation but also the unique structures of myxobacteria aggregates. It also suggests an explanation for the initialization of early aggregates, aggregation dynamics and final aggregate distribution.

We have shown that cells may use the noise of the population to their own advantage and have a high tolerance for making mistakes in the short run so that they can form the largest aggregates in the long run. We also demonstrate that streams play an important role in these processes and can perhaps be viewed as a form of long-range communication between cell aggregates. Despite the simplifications, the model makes a number of interesting predictions that can be experimentally tested.

2. Biological background

Myxobacteria cells are elongated, with a 2:1 to 14:1 length to width ratio, depending on the species, and are typically 2 to 12 μm by 0.7 to 1.2 μm (Reichenbach 1993). A myxobacteria cell glides by using two types of motility engines located at the cell poles: adventurous (A)-motility, in which cell secrete slime from the tail pole that hydrates and pushes the cell forward (Wolgemuth *et al* 2002), and social (S)-motility, in which pili extend from the cell head pole, attach to fibrils secreted by nearby cells, and then retract, pulling the cell forward (Kaiser 2000, Wolgemuth *et al* 2003).

Fruiting body development is controlled by the contact-mediated morphogen C-signal which is exchanged by cell–cell contact at cell poles (Kim and Kaiser 1990b, 1990c). Different levels of C-signal, encoded by the *csgA* gene, induce the different stages of fruiting body formation (Kim and Kaiser 1991, Li *et al* 1992). The expression of *csgA* is controlled by two feedback loops in the signal transduction pathway, one of which is caused by the increased density and alignment in response to the C-signal (Kim and Kaiser 1991, Li *et al* 1992, Jelsbak and Sjøgaard-Andersen 2002). The second is an

intracellular loop via the act operon (Gronewold 2001) so that each time a cell receives the C-signal it increases expression of *csgA*.

Myxobacteria cells do not divide during fruiting body formation, so cell motility is necessary for increases in cell density. Experimental evidence shows that cell motility is required to increase the levels of C-signal for fruiting body formation (Kim and Kaiser 1990b, 1990c). Also, cell motility results in cell alignment (Wolgemuth *et al* 2002, Buchard 1981) as cells make small (incremental) modifications in their direction of motion as they move. Increased cell density and alignment over time increase C-signaling such that the different stages are induced at the right times during development (Kim and Kaiser 1991, Li *et al* 1992, Kruse *et al* 2001).

Computational models based on C-signaling were first applied to explain myxobacteria rippling patterns (Igoshin *et al* 2001, Börner *et al* 2002, Lutscher and Stevens 2002, Alber *et al* 2004a). Rippling myxobacteria form a pattern of equi-distant ridges of high cell density that appear to travel periodically through the population. In computational models for rippling, head-on collisions between oriented cells initiate C-signaling that causes cell reversals. These models are based upon Sager and Kaiser's hypothesis of precise reflection (Sager and Kaiser 1994): when two wavefronts collide, the cells reflect one another, pair by pair, in a way that preserves the wave structure. A recent paper (Igoshin *et al* 2004) has extended an earlier model for rippling to include myxobacteria aggregation. Our model, described in Alber *et al* (2004b), complements the continuum model used in Igoshin *et al* (2004) and focuses on a two-stage aggregate formation via streams.

Several biological models have been proposed to explain myxobacteria aggregation (e.g. Dworkin 1996). Stevens (2000) described aggregation by cells following slime trails deposited by other cells. She demonstrated that slime-trail following alone (with cells depositing slime, gliding preferentially on slime tracks and gliding faster on slime tracks) could form unstable aggregation patterns that resembled experimental observations. Namely, aggregates would form, diffuse away and reappear in other regions. However, the simulation of stable centers was shown to require an extra factor such as a diffusing chemoattractant.

Sjøgaard-Andersen and Kaiser (1996) proposed that sequential end-to-end cell contacts and biased motion toward higher density aggregates result in the formation of streams leading into aggregates. In Jelsbak and Sjøgaard-Andersen (2002), this model is proposed as a mechanism for symmetry-breaking and aggregation in myxobacteria. Streams coalesce or turn in on themselves in spiral movements to form aggregates. Within an aggregate, cells move in circular tracks. This model predicts that aggregates remain unstable as long as cells are motile, because streams with straight rather than circular trajectories will drain the aggregate. However, experiments show that cells move faster within aggregates (Sager and Kaiser 1993).

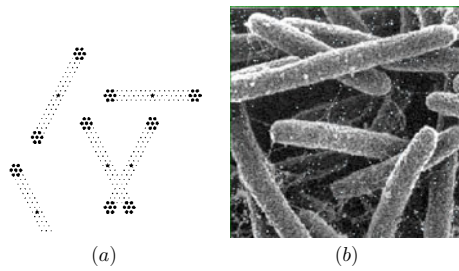


Figure 1. (a) Five simulation cells are shown on a 42×42 node lattice subsection. The cell's 'center of mass' is indicated by a star and the nodes of the interaction neighborhood where C-signal is exchanged are indicated by the larger black discs at the cell poles. (b) SEM image of (*Myxococcus xanthus*) cells in submerged culture (from Behmlander and Dworkin (1991) with permission).

3. Computational model

We model cell movement on a hexagonal lattice using a cellular model introduced in Alber *et al* (2004a). There are six allowed unit velocities (or *channels*) for each cell. We represent myxobacteria cells as (1) a single node which corresponds to the position of the cell's center (or 'center of mass') in the xy plane, (2) an occupied channel at the cell's position designating the cell's orientation and (3) a local neighborhood defining the physical size and shape of the cell with associated interaction neighborhoods. Cells move exactly one node per timestep in the direction of their orientation and, by a simple exclusion rule, there is only one cell center per channel per node. Myxobacteria cells are elongated during aggregation, so we model cells with width 3 and length 21 on a hexagonal lattice as shown in figure 1. Each cell has two distinct C-signaling neighborhoods: a head and a tail. C-signaling occurs when the C-signaling nodes at the head of a cell overlap with the C-signaling nodes at the tail of another cell.

The local rules for aggregation demand that cells turn by 60° or else persist in their original direction with probability favoring directions that would maximize C-signal exchange between cells. Myxobacteria turn by small angles as they move, which is accounted for by their motility systems (Kaiser, private communication). Myxobacteria cells also reverse; i.e., switch their motors between the cell poles so that the leading end of the cell becomes the lagging end, and vice versa (Kaiser 2003). Cell reversal is crucial in generating the rippling patterns preceding aggregation (Igoshin *et al* 2001, Börner *et al* 2002, Lutscher and Stevens 2002, Alber *et al* 2004a), but because the cell reversal frequency is significantly reduced in aggregation (Jelsbak and Søgaard-Andersen 2002), we do not consider cell reversals in this study.

Our model's local rules increase alignment because cells turning preferentially to the C-signal will arrange end-to-end. These local rules also increase cell density because cells preferentially turn into higher cell density areas where there is more C-signal. Thus, these local rules combine C-signaling with the increase in cell density and cell alignment. Additional local rules accounting for slime production and cell and slime adhesivity would presumably be required for modeling more subtle inter-species differences in myxobacteria.

4. Results and discussion

4.1. Early aggregation and aggregate structure

We compare early aggregate formation in simulation with that of the Kuner submerged culture experiment described in Kaiser and Welch (2004). In these experiments, cells do not form traveling waves (ripples) preceding aggregation.

In experiment, suspended myxobacteria cells settle in several layers randomly on a glass surface. The settled cells soon form ordered cellular domains (see figure 2(a)). We begin the simulation with ten layers of randomly oriented cells, which shortly turn into regular arrays as cells align by C-signaling (figure 2(d)).

In experiment, after the appearance of aligned patches, preliminary aggregates begin to form, usually at the boundary between patches where density is assumed to be high, figure 2(b) (Kaiser and Welch 2004). In simulation, cells in aligned arrays turn from low density areas toward areas of slightly higher cell density and then the cells condense into many closely spaced aggregates. In both experiment and simulation, aggregates grow as immediately surrounding cells enter the aggregate.

In simulation, depending on the aggregate size, aggregates form one of six distinctive types, shown in figure 3, ordered by increasing size. Very small, typically early, aggregates in our simulation have the characteristics of early developing *Myxococcus xanthus* aggregates. Early *Myxococcus xanthus* aggregates are asymmetric (figure 2(b)) and have been referred to as 'traffic jams', because it is assumed that cell motility is hindered by many cells trying to move in antagonistic directions (Kaiser and Welch 2004). Likewise, in simulations the directions of cells in initial aggregates of type I are disordered and cells are analogously 'jammed': tracking of cells in these aggregates has shown that cells rarely travel more than one quarter of a cell length before turning several times and entirely reversing their direction. Also, simulation aggregates round out as more cells are added to the aggregate (compare aggregates of type I with aggregates of type II–VI in figure 3), just as asymmetric aggregates in experiment grow and gain circular symmetry from 8 to 24 h (Kuner and Kaiser 1982).

Larger aggregates in our simulation have the unique structure of mature myxobacteria aggregates for several myxobacteria species. In *Myxococcus xanthus*, the basal region of the fruiting body is a shell of densely packed cells which orbit in two directions, both clockwise and counterclockwise, around an inner region only one-third as dense (Sager and Kaiser 1993, Julien *et al* 2000). A magnified picture of the cell centers of aggregate type II (figure 3 in our simulation shows that cells are arranged in a dense, concentric layer tangent to a relatively low-density inner region. Cell tracking shows that cells orbit either clockwise or anticlockwise along the periphery of the orbit. The fruiting bodies of myxobacteria often occur in fused clusters called sporangioles (for example, *S. erecta* (Reichenbach 1993)). Intermediate-sized aggregates in our simulation form in clusters of two or three closed orbits (III and IV in figure 3). The largest simulation aggregates (type V and

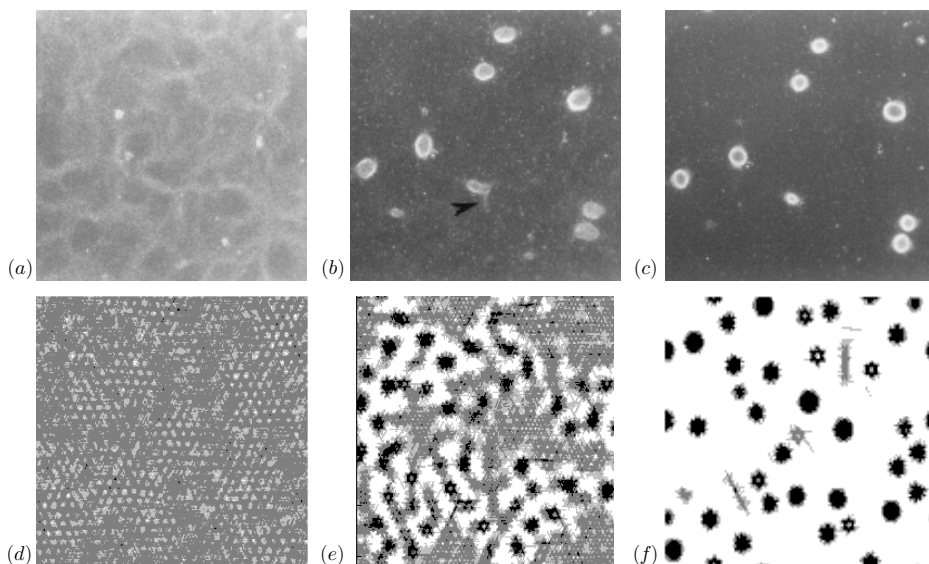


Figure 2. (a)–(c) Light microscopic images of *Myxococcus xanthus* during fruiting body aggregation stages in submerged culture of Kuner type, at 1 h, 11 h and 24 h, respectively. Field of view is about $4 \times 4 \text{ mm}^2$ (from Kaiser and Welch (2004) with permission). (d)–(f) Simulation of aggregation stages on a 500×500 lattice, which corresponds to an area of $2.8 \mu\text{m}^2$. Local cell density after (d) 25 timesteps, (e) 300 timesteps and (f) 25 000 timesteps. Initial cell density is 10. The number of simulated cells is 39 507. The darker shade of gray corresponds to higher cell density.

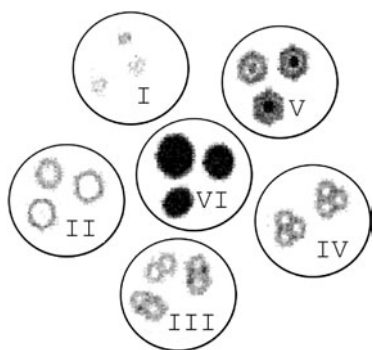


Figure 3. Six aggregate types, I–VI, ordered by increasing aggregate size, (aggregates identified within two simulations over 25 000 timesteps).

VI) have no hollow center. Presumably, modeling in three dimensions would be required to resolve their three-dimensional structure.

4.2. Stable attractor region in area–density phase space

Aggregate shape is size dependent. Given a fixed number of interacting cells in a stationary aggregate there is a unique structure chosen by the cells, and thus, a unique stable configuration. We measured the areas and densities of every stationary aggregate which appeared over the course of two simulations. Simulation aggregates fall within a narrow range in the area–density phase diagram shown in figure 4(a), illustrating that for an aggregate of a given cell number, its area and density are narrowly prescribed within this region, which we call an ‘attractor region’ because it appears to attract all aggregates. As simulation aggregates grow, their

shape modulates continuously from type I to type VI. These aggregate types occupy distinct regions by increasing area and density within the attractor region.

We perform two kinds of perturbations to test the stability of this region. First, we study an adiabatic perturbation by gradually adding cells to an initially small, isolated aggregate. As cells are slowly added, the aggregate increases in area and density while remaining within the attractor region (figure 4(b)). Second, we introduce a non-adiabatic perturbation by placing two duplicate aggregates in close proximity to each other, which creates a new aggregate with double the initial area and the same density (indicated by a star in the phase space in figure 4(c)). Over 600 timesteps, this aggregate gradually reorganizes so that it has an area and density within the region (figure 4(c)). Results from both kinds of perturbations suggest that this region is a stable attractor in the area–density phase space of aggregates.

4.3. Stream formation

Kaiser and Welch (2004) recently performed a detailed analysis of aggregate distribution in *Myxococcus xanthus* experiments. In the Kuner submerged culture, of 22 initial asymmetric aggregates tracked, only 13 remain over the course of the experiment. This trend is repeated in the submerged agar culture, in which 18 initial aggregates eventually reduce to three fruiting bodies. Likewise, in simulation only one out of three initial simulation aggregates remain at the end of simulations with standard initial density of ten cell layers. We find that thin streams of aligned cells have an important role in this final aggregate distribution.

Thin streams of cells have been observed in submerged agar culture (Kaiser and Welch 2004) and other experiments

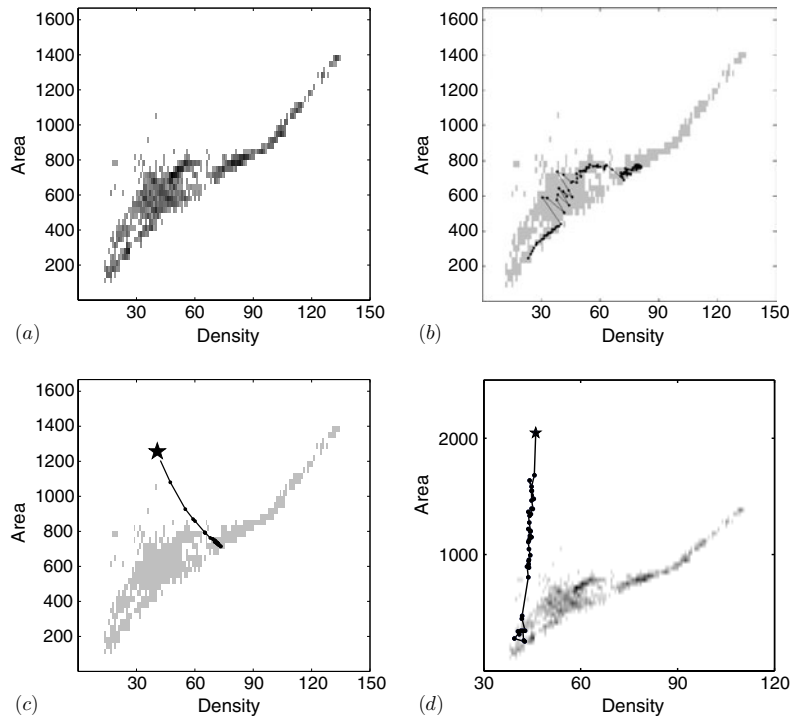


Figure 4. Area–density phase diagram for (a) 186 stationary aggregates identified within two simulations over 25 000 timesteps (b) an initially small aggregate to which cells are slowly added over 1000 timesteps (c) an artificially constructed aggregate (star) over 600 timesteps and (d) a simulation stream which decreases in size over 27 000 timesteps as it stochastically loses cells to nearby aggregates, until it eventually becomes a stable aggregate. Relaxation of perturbation data are plotted every 10 timesteps on a background of (a), while stream data are plotted every 500 timesteps.

(Kuhlweil and Reichenbach 1968, O’Connor and Zusman 1989). It has been suggested that streams bring cells to aggregates (Kuhlweil and Reichenbach 1968, O’Connor and Zusman 1989, Søgaard-Andersen and Kaiser 1996) and streams may be responsible for funneling cells from one aggregate to another (Kaiser, private communication). We find that streams form by C-signaling when aggregates crowd, and function to ensure a final distribution of large-sized aggregates in a robust two-stage mechanism. First, initial aggregation occurs as cells turn from low to higher density areas. Cells interact only with their neighbors through contact, thus this aggregation is limited to an area of a few cell lengths and results in the formation of many small aggregation centers. Second, long and thin streams form between small, closely spaced aggregates, allowing long-range communication between cells and redistributing cells from many small aggregates to fewer, larger aggregates (compare figures 2(e) and (f)).

In simulations, initial aggregates crowd as they grow. When the distance between aggregates is less than one cell length, adjacent aggregates begin exchanging cells. Due to C-signaling, the cells form end-to-end contacts that lead them to align in a stream. Cells in streams C-signal with the tails of cells ahead of them and the tails of cells moving past them. The width of a stream gets thinner to maximize C-signaling along the stream direction. The track of a single stream cell shows that it moves toward the end of the stream at the maximal velocity (without turning), then diffuses randomly once it has

left the stream. The cell continues to random-walk until it re-enters the stream by chance. It has changed direction, and progresses at the maximal velocity toward the other end of the stream. Most streams are oriented in one of the three lines defined by the hexagonal symmetry of the lattice (i.e., oriented at 0° , 60° or 120° with respect to the horizontal semi-axes). However, streams also occasionally form at directions halfway between the angles of the lattice, orienting at 30° , 90° or 150° with respect to the horizontal semi-axes. In these streams, cells adjust their direction by frequently turning one step clockwise and then one step counterclockwise so that their average direction is the intermediate lattice direction.

A new finding from our model is that streams form in regions influenced by two or more aggregates in close proximity. This result is supported by the observation of streams when *Myxococcus xanthus* aggregates develop in submerged agar culture. Transient streams are visible, always between adjacent aggregates (see figures 5(a) and (b)). Simulation streams formed between aggregates as shown in figures 5(c)–(e).

The area–density phase diagram described above not only prescribes the region of stable aggregates, it also helps us understand the formation of streams. When two stationary aggregates interact, the area of interacting cells increases at the moment of interaction while the density remains approximately the same. Thus, the newly formed aggregate lies off the attractor region. Large aggregates with high cell density and area will fuse and quickly form a new stationary

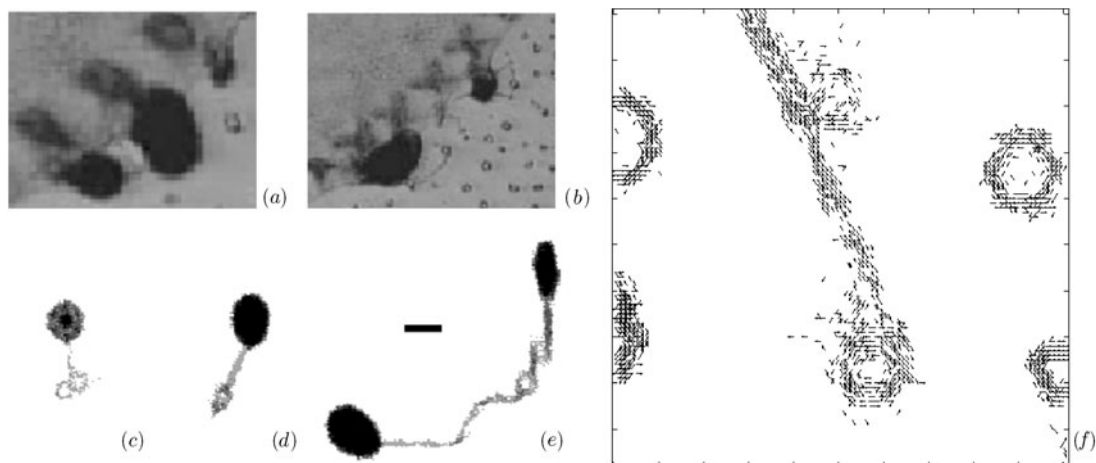


Figure 5. Streams form between *Myxococcus xanthus* aggregates on the edge of a submerged agar culture after (a) 28 and (b) 42 h after starvation (from Kaiser and Welch (2004) with permission). (c)–(e) Cells within typical simulation streams in which the initial cell density was 50 cell layers (black bar indicates one simulation cell length). (f) Direction of cell centers at 450 timesteps (100×100 node lattice subsection) showing two aggregates connected by a stream. Initial cell density was 10 cell layers.

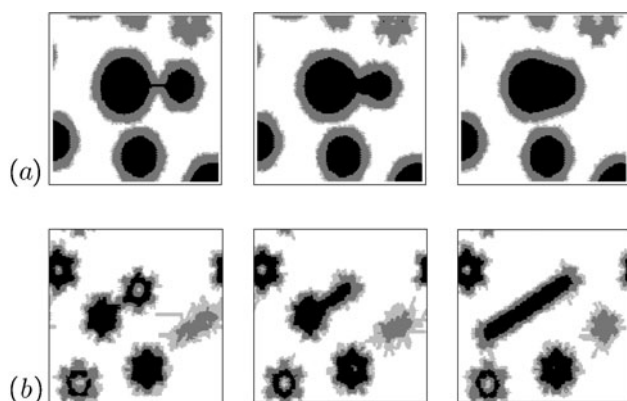


Figure 6. Two types of aggregate interaction on a 128×128 node lattice. (a) Two large aggregates fuse via a submerged stream. Panels left to right correspond to 19 000, 24 000 and 26 000 timesteps, respectively. (b) Two small aggregates form a stream. Panels left to right correspond to 900, 1000 and 1200 timesteps, respectively.

aggregate, as in figure 6(a). This type of aggregate interaction has been described in the area–density phase space in figure 4(c). Smaller aggregates have a lower cell density and lower cell C-signaling levels, so when small aggregates fuse, they have a longer transient stage and are more likely to form a stream. Figure 6(b) shows the formation of a stream from two interacting aggregates.

A stream is bi-directional, with cells flowing equally in both directions along the stream. Given the end-to-end contacts required for C-signaling, an infinitely long stream of cells flowing in two directions is obviously a stable arrangement. However, there is a fixed number of cells within simulation streams, and thus streams are of finite length. Cells at the end of streams do not C-signal in the open space; hence they will diffuse without any preferred direction. Although randomly diffusing cells often find their way back into the stream, some cells escape from the stream. Over time, the

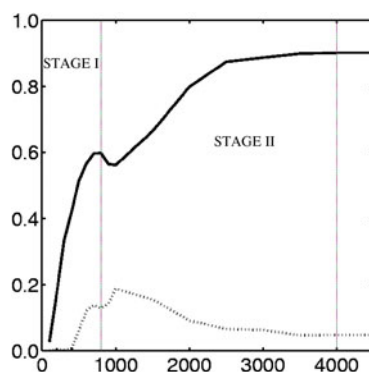


Figure 7. The fraction of cells within aggregates (solid lines) and within streams (dotted lines) for initial lattice density 10.

stream shortens as it gradually loses cells. Figure 4(c) shows the path of a simulation stream in the area–density phase space as it stochastically loses cells over time. A stream will lose cells more quickly if there is an aggregate near the end of the stream to absorb cells diffusing at the ends of the stream.

The fate of the stream tracked in area–density phase space in figure 4(d) is to become a small, stable aggregate. This occurs because a shortened stream is more sensitive to the noise caused by the cells freely diffusing at each end of the stream. After an abrupt and brief disordered transient state, the stream reorganizes into an aggregate. The area–density phase diagram enables a prediction of the final aggregate shape based on the number of cells within the stream.

4.4. Redistribution of cells within aggregates via streams

In simulation, during the second stage of aggregate formation, streams redistribute cells from many small aggregates to fewer, larger aggregates. The time-dependent role of streams can be seen by the fraction of cells found within stationary aggregates versus streams over time (figure 7). Initially cells join stationary aggregates and the fraction of cells

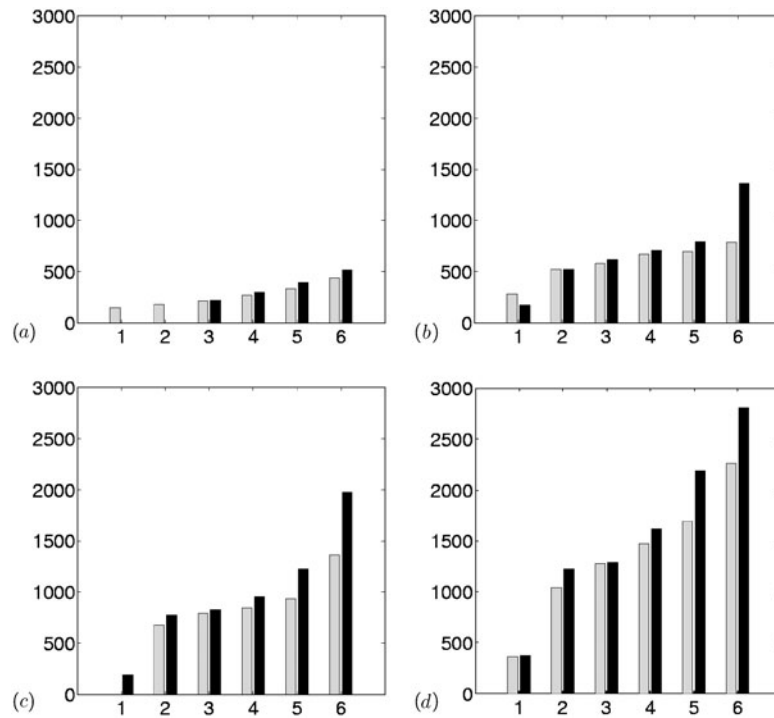


Figure 8. Aggregate size distribution at the beginning of stage II (gray bars) and at the end of stage II (black bars). Initial simulation densities (a)–(d) are 1, 10, 20 and 50. Shown are average aggregate sizes of each of six quartiles. These plots also show that aggregate size increased with density.

within aggregates increases monotonically, labeled stage I in figure 7. As stationary aggregates grow, they may begin interacting to form streams. Cells within streams are taken from the population of cells within stationary aggregates, causing a dip in the fraction of cells within stationary aggregates. Stage II of aggregate formation is the span of simulation time over which streams redistribute cells among aggregates. We define the beginning of stage II as when the first dip occurs in the fraction of cells in aggregates and the end of stage II as when 95% of cells are within stationary aggregates. During stage II, cells are distributed among fewer, larger aggregates.

4.5. Role of the initial cell density in redistribution of cells

In simulations, the redistribution of cells in stage II from many small aggregates to fewer, larger aggregates is most significant at intermediate initial cell densities (see figure 8). As density is increased in simulations, the distance between aggregates remains constant while the size and density of aggregates increases. At very low density, the set of initial aggregates does not grow as large. Thus, aggregates interact less often to form streams and, once formed, very small streams do not expand very far, and only shrink into small aggregates. At high cell density, very large, dense aggregates form. When these aggregates interact, they fuse into a larger aggregate without first expanding into a stream (see figure 6(a)). At intermediate cell density, the average aggregate size grows most from the beginning of stage II to the end of stage II. This is due to the effect of streams as more aggregates interact and form larger streams. The longest stream length is an important

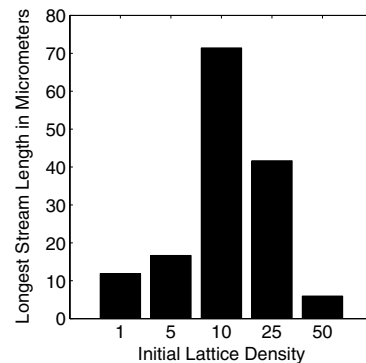


Figure 9. Relationship between initial number of cell layers (lattice density) and longest simulation stream length. Initial densities are 1, 5, 10, 25 and 50 from left to right.

variable because it determines the longest range of interaction between cells. The relationship between initial lattice density and longest stream length is summarized in figure 9.

4.6. Role of noise in enhancing effects of streams

Simulations with different random initial conditions develop very similarly. The standard deviation of lattice density increases with similar slope and to similar levels, indicating that pattern formation and simulation dynamics are not very sensitive to the noise from initial conditions.

The cell aggregation system is intrinsically noisy because cells turn at random with the preference for maximum C-signaling. How does this internal noise influence the

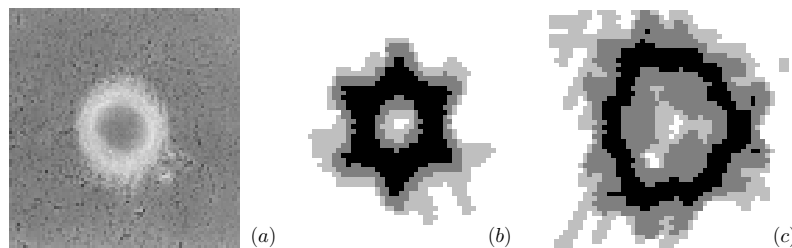


Figure 10. (a) An experimental aggregate in Kuner submerged culture at 24 h magnified with a $\times 16$ phase-contrast objective compared to the images in figures 2(a)–(c). From Kaiser and Welch (2004) with permission. Mature simulation aggregates of type II for persistence lengths (b) 1 and (c) 3 shown on identical 50×50 node lattice subsections.

aggregation? We have devised a corresponding deterministic model such that instead of using a stochastic process to model cell turning, we use the following function to determine the cell orientation for the next step:

$$f_i(r, k+1) = f_{i\ominus}(r - c_{i\ominus}, k)\Omega(r - c_{i\ominus}, k, c_i) \\ + f_{i\oplus}(r - c_{i\oplus}, k)\Omega(r - c_{i\oplus}, k, c_i) \\ + f_i(r - c_i, k)\Omega(r, k, c_i),$$

where f is the particle density distribution function over each lattice node r , k is the timestep, and c_i , $c_{i\ominus}$ and $c_{i\oplus}$ represent velocity vectors in the i th direction, vectors turning clockwise and counterclockwise from the i th direction, respectively. The collision function $\Omega(r, k, i)$ is the probability of a cell at the node r turning toward direction i at the k th timestep. We drop the exclusion principle so that the density of cells may be greater than 1 at a node. This function effectively converts our stochastic model based on cell turning into a deterministic model, analogous to the process of changing a stochastic lattice gas model to a deterministic lattice Boltzmann model (Frisch *et al* 1987).

Our simulations show that this deterministic model evolves similarly to the stochastic model, indicating that the aggregation dynamics are not sensitive to internal noise. As in the stochastic model, the deterministic model proceeds in stages. First, many small aggregates appear; then streams form between interacting aggregates until the streams dissolve and leave behind a larger set of aggregates. One important difference is that streams in the deterministic model are fewer and smaller. Another difference is that streams are shorter-lived, and the deterministic simulation reaches a steady state much faster. These differences have a critical effect on the way aggregates reorganize. Comparing the size distribution of aggregates in the stochastic model with that of the equivalent deterministic model (Alber *et al* 2004b), we see that with the internal noise, aggregates can reach larger sizes. This is not surprising because noise slows the process of stream contraction so that streams persist longer and span a greater area, which enables more aggregates to interact and eventually form larger, more stable aggregates.

4.7. Matching experimental spatial scales

Myxobacteria aggregates range in size between 10 and $1000 \mu\text{m}$ and are composed of 10^4 to 10^6 cells (Reichenbach 1993). The experimental figure shown in figure 2(c) (or

figure 1(e) in Kaiser and Welch (2004)) shows approximately 15 aggregates on a $4 \times 4 \text{ mm}$ subsection of a glass plate. Assuming a $1 \times 7 \mu\text{m}$ cell and initial cell density 10, modeling at this spatial scale would require simulating 25 million cells on a 12000×12000 lattice, well beyond our computational capabilities. In the simulations described in this paper, the spatial scale of aggregation is reduced to accommodate aggregate dynamics on a 500×500 node lattice. The distance between aggregates, which is independent of initial density, scales at $1/50$ compared to the distance between experimental aggregates and the largest simulation aggregates (at initial density 10) scale at $1/20$ compared to the largest experimental aggregate. For example, in the Kuner submerged culture experiment described in Kaiser and Welch (2004), early ordered cellular domains are approximately 0.2 to 0.4 mm (see figure 2(a)), while the patch-like arrays of aligned cells that form in simulation from random initial conditions are only 3 to 6 μm . Our largest simulation aggregates are only about 15 μm in diameter.

This reduction in the spatial and temporal scale of the aggregate pattern formation is accomplished by enabling simulation cells to turn frequently, much faster than the rate at which experimental cells can turn. We assume that the cell velocity is 7 μm per min and we represent a cell length of 7 μm by 21 nodes. Then, cells turning by 60° at each timestep can turn 60° every 3 s. Realistically, biological cells have a persistence time P , which is the average length of time between cell turns. Simulation cells are able to turn more frequently and quickly, so they organize into small aggregates spaced close together and follow an orbit with a very small radius of curvature.

To account for cell persistence time in our simulations, we can define a parameter P which represents the minimum number of timesteps a cell travels between turns. By increasing P , the spatial scales of pattern formation increase so that aggregates are larger (figure 10).

We find that as the persistence time is increased, the distance between aggregates increases. Without increasing the density, the aggregates eventually begin forming too far apart to interact and form streams. To model aggregate formation at a larger spatial scale, we propose including a small fraction (1–2%) of cells that do not move (peripheral cells). By secreting slime and thus enabling social motility, these cells could play a role in establishing more long-range communication by facilitating travel between aggregates.

5. Conclusion and outlook

The precise mechanism which determines positions and sizes of aggregation centers in fields of myxobacteria cells is unknown. Our simulations suggest a mechanism for the formation and position of aggregation centers through a two-stage process. During the short initial aggregation stage, any region has the potential to develop into an aggregation center. Cells join those aggregation centers as cells move by random walk. The distance between initial aggregates does not appear to depend on density, but depends sensitively on cell motility parameters. Streams then form between interacting aggregates resulting in fewer, larger aggregates, which will further develop into fruiting bodies.

Our cell aggregation model is based on a simple local rule whereby cells align by turning preferentially to make end-to-end contacts. This rule mimics C-signaling in myxobacteria, which drives myxobacteria aggregation. Cells in our model interact locally, while collectively they form streams and large aggregates. Streams and aggregates have different behaviors and roles even though they are composed of identical cells following identical rules. Large, stationary aggregates are most stable, while motile streams aid in large aggregate formation. Streams are most important for intermediate cell density. The presence of some internal noise enhances streaming and results in more efficient aggregation.

Despite its simplifications, our model makes a number of interesting predictions that can be experimentally tested. For the experiments suggested below, we assume that rippling is not a dominant collective behavior because there is little initial cell order, as in the submerged culture experiments of Kuner type described in Kaiser and Welch (2004).

Foremost among our predictions is the formation of streams between interacting aggregates. In experiments, one myxobacteria aggregate has been observed to grow as an adjacent aggregate disappears. Our model offers an explanation: a stream may form connecting two adjacent aggregates, and cells migrate from the smaller aggregate to the larger aggregate. These streams may not be visible in experimental movies due to low resolution. We predict that developing aggregates placed adjacent in experiment will fuse via a stream between the two aggregates if the initial aggregates are larger than a certain threshold size. If the initial aggregates are smaller than this threshold size, the aggregates will elongate upon interaction and form a stream, which will either merge into another aggregate or shrink into a small aggregate. If the aggregates are farther apart than a few cell lengths, aggregate fusion can be facilitated by smearing a line of cells from one aggregate to the other with a needle, and thus artificially forming a stream.

As evident from the attractor region in the area–density phase diagram, aggregate density increases with aggregate area, suggesting that for aggregate mounds without a stalk, aggregate height increases with aggregate area. This trend would be straightforward to verify in, e.g. *Myxococcus xanthus* simply by measuring the heights and areas of aggregates. If the experimental measurements also form a narrow attractor region in the height–area space, we can claim that our simple

cell model based on C-signaling captures some essence of myxobacteria aggregation. As real aggregates are 3D packing in continuous space, the simulations are 2D packing of cells on a hexagonal lattice so we should not expect a quantitative correspondence between the simulation and experimental attractor regions. In a 3D model extension, disc-shaped aggregates would correspond to hemispheres.

If experiments indeed confirm the existence of an attractor region, it would be interesting to test whether this region is as stable *in vivo* as it is in simulations. One would need to perturb an aggregate in experiment to see if it would relax to a position along the pre-determined curve. For example, two aggregates can be forced to fuse as described in figure 4(c), or cells can be slowly added to an aggregate (figure 4(b)), or the aggregate can be mechanically disturbed. These perturbations correspond to external noise in the system. The role of internal noise can be tested experimentally by transiently or permanently increasing the level of noise in the cell population. The level of noise can be increased transiently by spraying the population with a layer of randomly oriented cells, as the cells would align over time with the original layers of cells. Adding detergent-solubilized exogenous C-signal to the cell population as in Sager and Kaiser (1994) or adding cells which produce C-signal but which are unresponsive to C-signal would permanently increase the level of internal noise. Our model predicts that with increased internal noise, more streams would form and streams would last longer.

Another interesting set of experiments would be to investigate the effect of a change in initial cell density by regulating the initial amount of C-signal in the cell aggregates. For example, total C-signaling can be decreased by diluting a wild-type population with non-C-signaling cells as in the experiments described in Sager and Kaiser (1994), which has the effect of decreasing the density of C-signaling cells. As cell density is increased in simulations from nearly zero levels, there is a gradual change in the observed behavior. At the lowest initial cell densities, developing aggregates in simulations are small compared to the distance between them and fail to interact and form streams. As the initial density increases, larger aggregates form closer together and are likely to interact to form streams. At much higher initial densities, interacting aggregates immediately fuse rather than form streams. For different C-signaling levels, we predict a difference in aggregate size distributions qualitatively like figure 8, and that observed stream lengths will be greatest at intermediate initial densities.

Our simulations demonstrate that patterns analogous to experimental myxobacteria aggregates may arise from C-signaling based on simple local rules implemented in our discrete model on a hexagonal lattice. A discrete model has the advantage of enabling detailed analysis of individual cell behavior, which is especially appropriate for understanding a mechanism based on cell–cell contacts. However, the hexagonal lattice does introduce artifacts. For example, the limited number of directions permitted on a hexagonal lattice results in an overly regular pattern. At the control initial cell density (10 cell layers), developing aggregates have a hexagonal rather than spherical shape and streams are rigidly

straight. The hexagonal lattice and our simple local rules which allow turning by 60° at each timestep enable cells to follow a circular orbit with a very small radius of curvature. At lower initial cell density, the effect of these limitations is more pronounced. At high cell density these limitations have much less effect, when aggregates are spherical or even smoothly oblong and streams may curve smoothly over space. Although there are only six directions on the lattice, streams can form in 12 directions.

Also, our model does not account for species-specific local rules. Myxobacteria fruiting bodies vary widely depending on species. Differences in fruiting body structure among different myxobacteria species may depend upon cell aspect ratio, varying adhesivity molecules, and relative roles of the A-motility and S-motility (Kaiser, private communication).

Kaiser and Welch (2004) have provided detailed observations in *Myxococcus xanthus* and proposed that ‘traffic jams’ stall cells and results in aggregation. Our model based on cell contact, movement and directionality does not include hard-body interactions between cells. This enables us to project many layers of cells onto a 2D lattice. However, a more sophisticated model, which is currently being tested, that includes a rule for a cell’s exclusion volume will be able to account for the important effects of cell jamming and will be able to resolve the three-dimensional structure of aggregates.

Acknowledgments

This work was supported by NSF grant no IBN-0083653 and by DOE under contract W-7405-ENG-36. We acknowledge support from the Center for Applied Mathematics and the Interdisciplinary center for the Study of Biocomplexity at the University of Notre Dame. We also thank Professors Dale Kaiser and Alex Mogilner for fruitful discussions.

Glossary

Adiabatic perturbation. A secondary influence on a system that is applied slowly and incrementally so that the system responds fast compared to the time-scale at which the influence is applied.

Alignment. In myxobacteria, rod-shaped cells arrange themselves parallel to each other.

Attractor region. A region in phase space that the dynamical system can enter but not leave, and which contains no smaller such region.

C-signal. A cell envelope-associated protein, encoded by the *csgA* gene, that is exchanged by contact at cell poles.

C-signaling. The contact-mediated signaling between myxobacteria cells.

Cellular automaton. A dynamic system that is discrete both in time and space, whose behavior is completely specified in terms of local interactions.

Channel. On the hexagonal lattice, the center of mass of each cell may move at unit velocity in six directions, or six channels.

Chemotaxis. The phenomenon in which bacteria, other organisms, or single cells of multicellular organisms direct their movements according to certain long-range chemical signals in their environment.

Fruiting body. A specialized structure in bacteria that produces spores.

Local rule. In cellular automata models, a local rule is a standard procedure by which the states on each lattice site are updated.

Myxobacteria. A special class of Gram-negative rod-shaped bacterium which glide on surfaces along their long axis. Under starvation conditions, it undergoes a developmental process in which roughly 100 000 individual cells aggregate to form a structure called the fruiting body over the course of several hours.

Phase space. Phase space is the collection of possible states of a dynamical system. Implicit in the notion is that a particular state in phase space specifies the system completely; it is all one needs to know about the system to have complete knowledge of the immediate future.

Stream. One of the stages during the fruiting body formation in myxobacteria, when a group of cells move in the same direction for an extended period.

Wild-type. The standard, normally-functioning phenotype of an experimental organism, often the one which occurs most frequently in nature.

References

- Alber M S, Jiang Y and Kiskowski M A 2004a Lattice gas cellular automaton model for rippling and aggregation in myxobacteria *Physica D* **191** 343–58
- Alber M S, Kiskowski M A, Glazier J A and Jiang Y 2003 On cellular automaton approaches to modeling biological cells *Mathematical Systems Theory in Biology, Communication and Finance* ed J Rosenthal and D S Gilliam (IMA vol 134) (New York: Springer) pp 1–39
- Alber M S, Kiskowski M A and Jiang Y 2004b Two-stage aggregate formation via streams in myxobacteria *Phys. Rev. Lett.* **93** 068102
- Behmlander R M and Dworkin M 1991 Extracellular fibrils and contact-mediated cell interactions *Myxococcus xanthus J. Bacteriol.* **173** 7810–21
- Ben-Jacob E, Cohen I and Levine H 2000 Cooperative self-organization of microorganisms *Adv. Phys.* **49** 395–554
- Boon J, Dab D, Kapral R and Lawniczak A 1996 Lattice gas automata for relative systems *Phys. Rep.* **273** 55–147
- Börner U, Deutsch A, Reichenbach H and Bär M 2002 Rippling patterns in aggregates of myxobacteria arise from cell–cell collisions *Phys. Rev. Lett.* **89** 078101
- Brenner M P, Levitov L S and Budrene E O 1998 Physical mechanisms for chemotactic pattern formation by bacteria *Biophys. J.* **74** 1677–93

- Buchard R P 1981 Gliding motility of prokaryotes: ultrastructure, physiology and genetics *Ann. Rev. Microbiol.* **35** 497–529
- Dworkin M 1996 Recent advances in the social and developmental biology of the myxobacteria *Microbiol. Rev.* **60** 70–102
- Frisch U, d'Humières D, Hasslacher B, Lallemand P, Pomeau Y and Rivet J P 1987 Lattice gas hydrodynamics in two and three dimensions *Complex Syst.* **1** 649–707
- Gronewold T M A and Kaiser D 2001 The act operon controls the level and time of C-signal production for *Myxococcus xanthus* development *Mol. Microbiol.* **40** 744–56
- Hagen D, Bretscher A and Kaiser D 1978 Synergism between morphogenetic mutants of *Myxococcus xanthus* *Dev. Biol.* **64** 284–96
- Heberlein U, Wolff T and Rubin G 1993 The TGF- β homolog dpp and the segment polarity gene hedgehog are required for propagation of a morphogenetic wave in the *Drosophila retina*. *Cell* **75** 913–26
- Hodgkin J and Kaiser D 1979 Genetics of gliding motility in *Myxococcus xanthus* (Myxobacterales): genes controlling movement of single cells *Mol. Gen. Genet.* **171** 167–76
- Hodgkin J and Kaiser D 1979 Genetics of gliding motility in *Myxococcus xanthus* (Myxobacterales): genes controlling movement of single cells *Mol. Gen. Genet.* **171** 177–91
- Höfer T, Sherratt J A and Maini P K 1995 Dictyostelium discoideum—cellular self-organization in an excitable biological medium *Proc. R. Soc. B* **259** 249–57
- Igoshin O A, Mogilner A, Welch R D, Kaiser D and Oster G 2001 Pattern formation and traveling waves in myxobacteria: theory and modeling *Proc. Natl Acad. Sci. USA* **98** 14913–18
- Igoshin O A, Welch R, Kaiser D and Oster G 2004 Waves and aggregation patterns in myxobacteria *Proc. Natl Acad. Sci. USA* **101** 4256–61
- Jelsbak L and Sogaard-Andersen L 2002 Pattern formation by a cell surface-associated morphogen in *M. xanthus*. *Proc. Natl Acad. Sci. USA* **99** 2032–37
- Julien B, Kaiser D and Garza A 2000 Spatial control of cell differentiation in *Myxococcus xanthus*. *Proc. Natl Acad. Sci. USA* **97** 9098–103
- Kaiser D 2000 Bacterial motility: how do pili pull? *Curr. Biol.* **10** R777–80
- Kaiser D 2003 Coupling cell movement to multicellular development in myxobacteria. *Nat. Rev. Microbiol.* **1** 46–54
- Kaiser D and Welch R 2004 Dynamics of fruiting body morphogenesis *J. Bacteriol.* **186** 919–27
- Kim S K and Kaiser D 1990a C-factor: a cell–cell signaling protein required for fruiting body morphogenesis of *M. xanthus* *Cell* **61** 19–26
- Kim S K and Kaiser D 1990b Cell motility is required for the transmission of C-factor, an intercellular signal that coordinates fruiting body morphogenesis of *Myxococcus xanthus*. *Genes Dev.* **4** 896–904
- Kim S K and Kaiser D 1990c Cell alignment required in differentiation of *Myxococcus xanthus*. *Science* **249** 926–28
- Kim S K and Kaiser D 1991 C-factor has distinct aggregation and sporulation thresholds during *Myxococcus development* *J. Bacteriol.* **173** 1722–28
- Kim S K, Kaiser D and Kuspa A 1992 Control of cell density and pattern by intercellular signaling in *Myxococcus* development *Ann. Rev. Microbiol.* **46** 117–39
- Komoto A, Hanaki K, Maenosono S, Wakano J Y, Yamaguchi Y and Yamamoto K 2003 Growth dynamics of *Bacillus circulans* colony *J. Theor. Biol.* **225** 91–97
- Kruse T, Lobedanz L, Berthelsen N M S and Sogaard-Andersen L 2001 C-signal: a cell surface-associated morphogen that induces and co-ordinates multicellular fruiting body morphogenesis and sporulation in *Myxococcus xanthus*. *Mol. Microbiol.* **40** 156–68
- Li S, Lee B and Shimkets L J 1992 csgA expression entrains *Myxococcus xanthus* development *Genes. Dev.* **6** 401–10
- Lobedanz S and Sogaard-Andersen L 2003 Identification of the C-signal, a contact-dependent morphogen coordinating multiple developmental responses in *Myxococcus xanthus*. *Genes Dev.* **17** 2151–61
- Lutscher F and Stevens A 2002 Emerging patterns in a hyperbolic model for locally interacting systems *J. Nonlinear. Sci.* **12** 619–40
- Martiel J and Goldbeter A 1987 A model based on receptor desensitization for cyclic AMP signaling in *Dictyostelium* cells. *Biophys. J.* **52** 807–28
- Matsushita M and Fujikawa H 1990 Diffusion-limited growth in bacterial colony formation *Physica A* **168** 498–506
- O'Connor K A and Zusman D R 1989 Patterns of cellular interactions during fruiting body formation in *Myxococcus xanthus* *J. Bacteriol.* **171** 6013–24
- Reichenbach H 1993 Biology of the myxobacteria: ecology and taxonomy *Myxobacteria II*. ed M Dworkin and D Kaiser (Washington, DC: American Society for Microbiology) pp 13–62
- Sager B and Kaiser D 1993 Two cell-density domains within the *Myxococcus xanthus* fruiting body *Proc. Natl Acad. Sci. USA* **90** 3690–94
- Sager B and Kaiser D 1994 Intercellular C-signaling and the traveling waves of *Myxococcus*. *Genes Dev.* **8** 2793–804
- Sogaard-Andersen L and Kaiser D 1996 C factor, acell-surface-associated intercellular signaling protein, stimulates the cytoplasmic Frz signal transduction system in *Myxococcus xanthus* *Proc. Natl Acad. Sci. USA* **93** 2675–79
- Stevens A 2000 A stochastic cellular automaton modeling gliding and aggregation of myxobacteria *SIAM J. Appl. Math.* **61** 172–82
- Tsimring L, Levine H, Aranson I, Ben-Jacob E, Cohen I, Shochet O and Reynolds W N 1995 Aggregation patterns in stressed bacteria *Phys. Rev. Lett.* **75** 1859–62
- Wakano J Y, Maenosono S, Komoto A, Eiha N and Yamaguchi Y 2003 Self-organised pattern formation of a bacteria colony modeled by a reaction diffusion system and nucleation theory *Phys. Rev. Lett.* **90** 258102
- Wolgemuth C, Hoiczky E, Kaiser D and Oster G 2002 How myxobacteria glide. *Curr. Biol.* **12** 369–77
- Wolgemuth C, Igoshin I and Oster G 2003 The motility of mollicutes *Biophys. J.* **85** 828–42